Polymer 51 (2010) 968–974

Contents lists available at ScienceDirect

Polymer

journal homepage: www.elsevier.com/locate/polymer

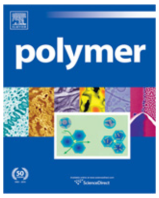

Relation between molecular orientation and morphology of a multiblock copolymer melt confined in cylindrical nanopores

Houyang Chen, Eli Ruckenstein*

Department of Chemical and Biological Engineering, State University of New York at Buffalo, Buffalo, NY 14260-4200, USA

ARTICLE INFO

Article history:
Received 26 October 2009
Received in revised form
23 December 2009
Accepted 5 January 2010
Available online 14 January 2010

Keywords:
Molecular orientation
Multiblock copolymer
Nanopore

ABSTRACT

The morphologies of multiblock copolymer melts (for simplicity, we consider tetra blocks) and their configurations when they are confined in cylindrical nanopores were examined by Lattice Monte Carlo simulations. The dependence of their morphologies and of the configurations of the copolymers (through the radius of gyration) on the nanopore diameter, intersegment interaction energies (repulsive interaction energies between different kinds of segments of the copolymers), and attractive interactions between one kind of segments and the surface of the nanopore was investigated. The results indicate that the morphology of a copolymer melt is connected to the configuration of the copolymer chain. It was found that: (i) stacked disks are generated when the polymer chains are preferentially directed along the nanopore axis, and (ii) helixes or lamellae parallel to the nanopore axis are formed when the copolymer chains are preferentially directed normal to the nanopore axis.

1. Introduction

Recently, a large number of reports on the self-assembly of diblock or triblock copolymer melts and copolymer solutions confined in cylindrical nanopores were published [1–21]. Obviously, the tetrablock copolymer melts which are of interest in the present paper exhibit more complex morphologies than the di- or triblock copolymers. The linear tetrablock copolymer Poly(styrene-*block*-isoprene-*block*-dimethylsiloxane-*block*-2-vinylpyridine), generates a four-phase triple coaxial cylindrical microdomain morphology [22]. A four-phase six-layer lamellar structure (–(ABCDCB)$_n$–) was obtained from Poly(isoprene-*block*-styrene-*block*-2-vinylpryidine-*block*-4-trimethylsilylstyrene) and identified by both Transmission Electron Microscopy and small angle X-ray scattering [23]. Jaffer et al. [24] investigated, by employing a self-consistent mean-field theory, the phase behavior of ABCD tetrablock copolymer melts. They found a noncentrosymmetric (NCS) lamellar phase (with the sequence …ABCDABCD…) in some regions of the phase diagram. Two partially mixed centrosymmetric (MCS) lamellar phases were also identified during the disordered to fully ordered phase transition.

All the above studies have shown that the morphologies of multiblock copolymers are more complex and only few papers have been concerned with them. In addition, the relation between the morphology of a block copolymer confined in a nanopore and its molecular configuration was not examined. If a relation between the morphology of a block copolymer and its molecular configuration could be established, it may help in the design of the morphology of block copolymers. The present paper has the goal to examine the connection between the molecular orientation and the morphology of the ABCD tetrablock copolymer melts. The effects of the nanopore diameter, of the repulsive interaction energies between different kinds of segments of the copolymer, and of the attractive interactions between one kind of segments and the wall of the nanopore on the morphologies of the tetrablock copolymer melts and the configurations of the copolymers are investigated.

This paper is organized as follows. In Section 2, some details on the Monte Carlo simulations are provided. In Section 3, the dependencies of the morphologies of the copolymer melts and configurations of the copolymer on the repulsive interactions between different kinds of segments, the attractive interactions between the segments and the wall of the nanopore, and on the nanopore diameter are explored. Then, the connection between the morphology and the molecular alignment is examined. The last section summarizes the conclusions.

2. Simulation details

The bond fluctuation model [25] and the volume diffusion algorithm [26] were employed in the Lattice Monte Carlo simulations employed in this paper. Each attempted motion either kept the bond length fixed or changed the bond length from 1σ to $\sigma\sqrt{2}$ or

---

* Corresponding author.
E-mail addresses: houyangchen2008@hotmail.com (H. Chen), feaeliru@buffalo.edu (E. Ruckenstein).

0032-3861/$ – see front matter © 2010 Elsevier Ltd. All rights reserved.
doi:10.1016/j.polymer.2010.01.002

in the opposite direction (σ being the lattice parameter) in the bond fluctuation model; the vacancy governed the motion in the volume diffusion algorithm. For more details one can see References [25–27]. The simulations were performed in a canonical ensemble. Each lattice point was occupied either by a segment (A, B, C, or D) or by a vacancy. All the attempted motions followed the excluded volume rule, the no-bond-crossing, and the above bond length restrictions. Any attempted motion was considered as accepted or rejected by using the traditional Metropolis algorithm.

The tetrablock copolymer $A_5B_5C_5D_5$, which posseses two outer blocks, A_5 and D_5, and two inner blocks, B_5 and C_5, with a volume fraction of 0.952 was considered. The remaining volume is occupied by vacancies which are involved in the volume diffusion algorithm. The length l of the nanopore (in the y direction) was 84σ. The diameter d of the cylindrical nanopore was varied between 9 and 29σ. In each simulation, we used 1.0×10^7 Monte Carlo steps to ensure that the final structures were stable. Only the interactions between the nearest neighbor segments were taken into account. The interaction between the same kinds of segments was considered zero, i.e. $\varepsilon_{AA} = \varepsilon_{BB} = \varepsilon_{CC} = \varepsilon_{DD} = \varepsilon_{SS} = 0$, but the interactions between different kinds of segments, ε_{AB}, ε_{AC}, ε_{AD}, ε_{BC}, ε_{BD}, ε_{CD}, and between one kind of segments (A or B) and the surface of nanopore,

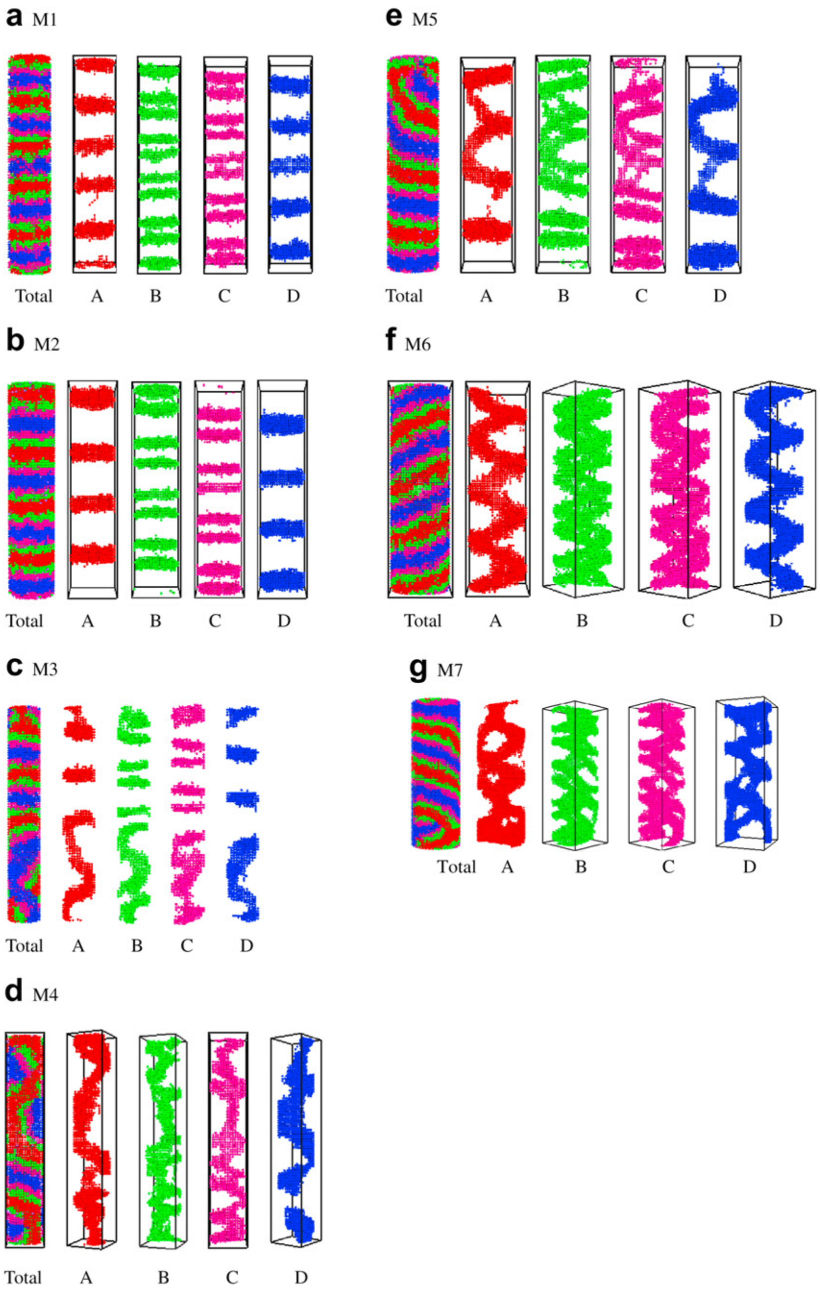

Fig. 1. Representative nanostructures in ABCD tetrablock polymer melts. (a) M1: ABCDDCBA alternate stacked disks with the period $L_p = 16.8\sigma$; (b) M2: ABCDDCBA alternate stacked disks with the period $L_p = 21\sigma$; (c) M3: mixed structure of ABCDDCBA alternate stacked disks and single helixes of each of the A,B,C,D segments; (d) M4: single helixes of each of the A,B,C,D segments; (e) M5: mixed structure of alternate stacked disks (with the sequence ABCDDCBA) + single helixes of each of the A and D segments + double helixes of each of the B and C segments; (f) M6: single helixes of each of the A and D segments + double helixes of each of the B and C segments; (g) M7: double helixes of each of the A,B,C,D segments. Red: A component; green: B component; pink: C component; and blue: D component. In each subfigure, from left to right, the morphologies are: total morphology of copolymer melts, morphology of A segments, morphology of B segments, morphology of C segments, morphology of D segments. (For interpretation of the references to colour in this figure legend, the reader is referred to the web version of this article).

ε_{AW} and ε_{BW},were varied. The interactions between the vacancies and the segments, and those between the segments C and D and the nanopore surface, were considered zero. Here, A, B, C and D stand for the segments A, B, C and D, S for the vacancies, and W for the surface of the nanopore.

3. Results and discussion

3.1. Neutral surfaces

Fig. 1 present seven kinds of microphase morphologies of the linear tetrablock copolymer $A_5B_5C_5D_5$ for a neutral nanopore. They are: the centrosymmetric stacked disks phase with the sequence ABCDDCBA and the length L_p of the repeat unit of stacked disks = 16.8σ(M1); the centrosymmetric stacked disks phase with the sequence ABCDDCBA and the period $L_p = 21\sigma$(M2); the mixed structure of alternate stacked disks with the sequence ABCDDCBA and single helixes of each of the segments A,B,C,D(M3); the single helixes of each of the A,B,C,D segments(M4); the mixed structure of alternate stacked disks (with the sequence ABCDDCBA) plus single helixes of each of the A and D segments plus double helixes of each of the B and C segments (M5); single helixes of each of the A and D segments plus double helixes of each of the B and C segments(M6); and double helixes of each of the segments A,B,C,D (M7). The calculations have been carried out for $\varepsilon_{AB} = \varepsilon_{AC} = \varepsilon_{AD} = \varepsilon_{BC} = \varepsilon_{BD} = \varepsilon_{CD} = \varepsilon$, $\varepsilon_{AA} = \varepsilon_{BB} = \varepsilon_{CC} = \varepsilon_{DD} = \varepsilon_{SS} = 0$, $\varepsilon_{AS} = \varepsilon_{BS} = \varepsilon_{CS} = \varepsilon_{DS} = \varepsilon_{WS} = 0$, $\varepsilon_{AW} = \varepsilon_{BW} = \varepsilon_{CW} = \varepsilon_{DW} = 0$, and $l = 84\sigma$. The morphologies of the tetrablock copolymer $A_5B_5C_5D_5$ melts for various pore diameters and repulsive energy ε are presented in Fig. 2. For diameters in the range considered in this paper (9–29σ), and at low repulsive interaction energies between different kinds of segments (e.g. $\varepsilon = 0.05kT$), the systems are disordered. As the repulsive interaction energy between different kinds of segments increases, ordered phases are formed, and an order–disorder transition (ODT) occurs at about $\varepsilon \approx 0.10kT$. The first ordered phase has a centrosymmetric structure (ABCDDCBA) with alternate stacked disks with the period $L_p = 16.8\sigma$. In this ordered phase, the A and D blocks are located at the head and the end of the tetrablock polymer, whereas the B and C blocks are located in the middle. Centrosymmetric structures of the ABCD tetrablock copolymers have been observed experimentally in bulk by Takano et al. [23] and predicted theoretically by Jaffer et al. [24]. A similar phase, consisting of ABCCBA alternate stacked disks, was found in triblock copolymers confined in cylindrical nanopores by Feng and Ruckenstein [15]. Takano et al. suggested [23] that such a morphology (i.e. alternate stacked disks with the sequence ABCDDCBA) consisted of a head-to-head alignment of ABCD molecules. Our simulations confirm their suggestion (Fig. 3). For the small diameters $d = 9\sigma$ and $d = 11\sigma$, an increase in the repulsive interaction energy transformed a part of the alternate stacked disks into single helixes for ε equal or larger than about 0.35kT. For $d = 13\sigma$, as the repulsive energy increases, the phase changes from a disordered to stacked disks, to mixed alternate stacked disks (with the sequence ABCDDCBA) and

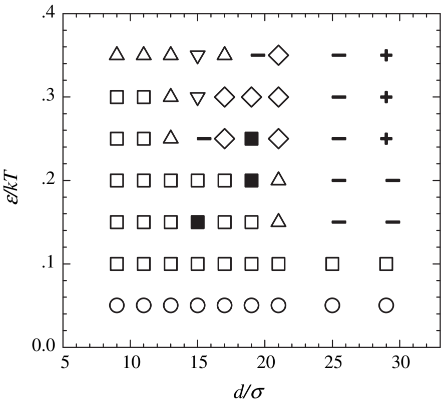

Fig. 2. Effects of interaction energy and diameter of nanopore on the morphology of the tetrablock copolymer $A_5B_5C_5D_5$ melts for $\varepsilon_{AB} = \varepsilon_{AC} = \varepsilon_{AD} = \varepsilon_{BC} = \varepsilon_{BD} = \varepsilon_{CD} = \varepsilon$, $\varepsilon_{AA} = \varepsilon_{BB} = \varepsilon_{CC} = \varepsilon_{DD} = \varepsilon_{SS} = 0$, $\varepsilon_{AS} = \varepsilon_{BS} = \varepsilon_{CS} = \varepsilon_{DS} = \varepsilon_{WS} = 0$, $\varepsilon_{AW} = \varepsilon_{BW} = \varepsilon_{CW} = \varepsilon_{DW} = 0$,and $l = 84\sigma$. Circle: Disordered Phase; Square, hollow: M1; Square, solid: M2; Triangle Up: M3; Triangle Down: M4; Diamond: M5; Horizontal mark: M6; Crosshair: M7.

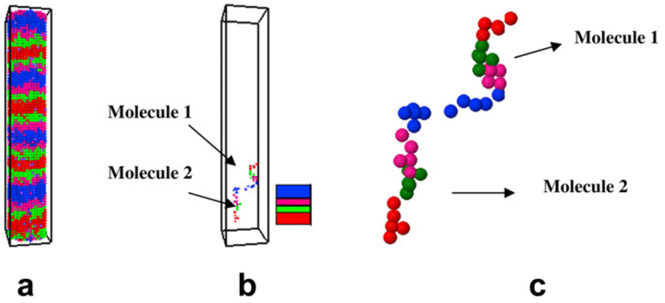

Fig. 3. Snapshots of the morphologies of the tetrablock copolymer $A_5B_5C_5D_5$ melt for $\varepsilon_{AB} = \varepsilon_{AC} = \varepsilon_{AD} = \varepsilon_{BC} = \varepsilon_{BD} = \varepsilon_{CD} = \varepsilon = 0.15\,kT$, $\varepsilon_{AA} = \varepsilon_{BB} = \varepsilon_{CC} = \varepsilon_{DD} = \varepsilon_{SS} = 0$, $\varepsilon_{AS} = \varepsilon_{BS} = \varepsilon_{CS} = \varepsilon_{DS} = \varepsilon_{WS} = 0$, $\varepsilon_{AW} = \varepsilon_{BW} = \varepsilon_{CW} = \varepsilon_{DW} = 0$, $l = 84\sigma$, and $d = 15\sigma$. (a) morphology; (b) two typical head-to-head (or tail-to-tail) alignment of ABCD molecules; (c) enlarged two molecules of (b).

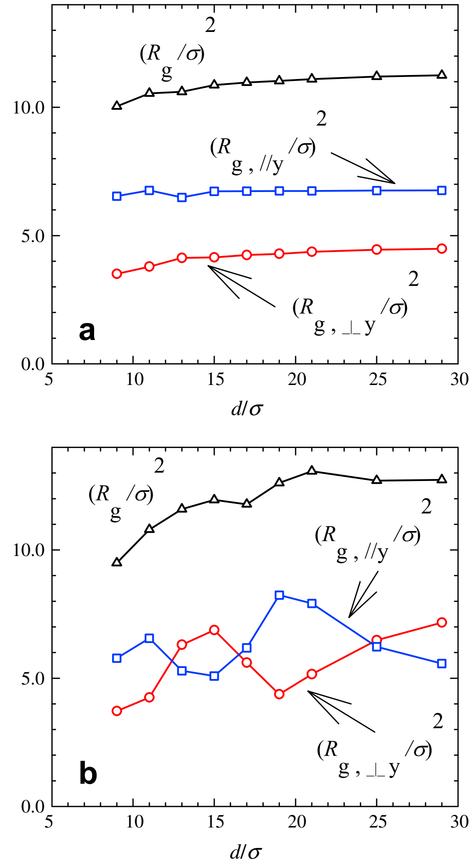

Fig. 4. Square radius of gyration of $A_5B_5C_5D_5$ for $\varepsilon_{AB} = \varepsilon_{AC} = \varepsilon_{AD} = \varepsilon_{BC} = \varepsilon_{BD} = \varepsilon_{CD} = \varepsilon$, $\varepsilon_{AA} = \varepsilon_{BB} = \varepsilon_{CC} = \varepsilon_{DD} = \varepsilon_{SS} = 0$, $\varepsilon_{AS} = \varepsilon_{BS} = \varepsilon_{CS} = \varepsilon_{DS} = \varepsilon_{WS} = 0$, $\varepsilon_{AW} = \varepsilon_{BW} = \varepsilon_{CW} = \varepsilon_{DW} = 0$, and $l = 84\sigma$.(a) $\varepsilon = 0.10kT$; (b) $\varepsilon = 0.25kT$.

single helixes of each of the A,B,C,D segments. The mixed structure of alternate stacked disks (with the sequence ABCDDCBA) and single helixes of each of the A,B,C,D segments were formed for ε equal or larger than about 0.25kT. For the diameters $d = 15\sigma$, $d = 17\sigma$, and $d = 19\sigma$, the alternate stacked disks (with the sequence ABCDDCBA) were changed into another of the ordered phases of Fig. 1 for ε equal or larger than about 0.25kT. The successive ordered phases are: the mixed structure of alternate stacked disks (with the sequence ABCDDCBA) and single helixes of each of the A,B,C,D segments; the single helixes of each of the A,B,C,D segments; the mixed structure of alternate stacked disks (with the sequence ABCDDCBA) plus single helixes of each of the A and D segments plus double helixes of each of the B and C segments; and the single helixes of each of the A and D segments plus double helixes of each of the B and C segments. For large diameters, such as $d = 21\sigma$, $d = 25\sigma$, and $d = 29\sigma$, and for ε equal or larger than about 0.15kT, the alternate stacked disks (with the sequence ABCDDCBA) transformed into another of the ordered phases mentioned above. A new kind of ordered phase, namely double helixes for each of the A,B,C,D segments, were formed for $d = 29\sigma$. These results indicate that the morphologies of the tetrablock copolymers depend on both the diameter of the nanopores and the repulsive interaction energy. For small nanopore diameters, there are fewer morphologies than for the large pore diameters. In other words, a “confining effect” is present in the nanopores of small diameters. As the nanopore diameter increases, the critical interaction energy for the transition from an ordered centrosymmetric

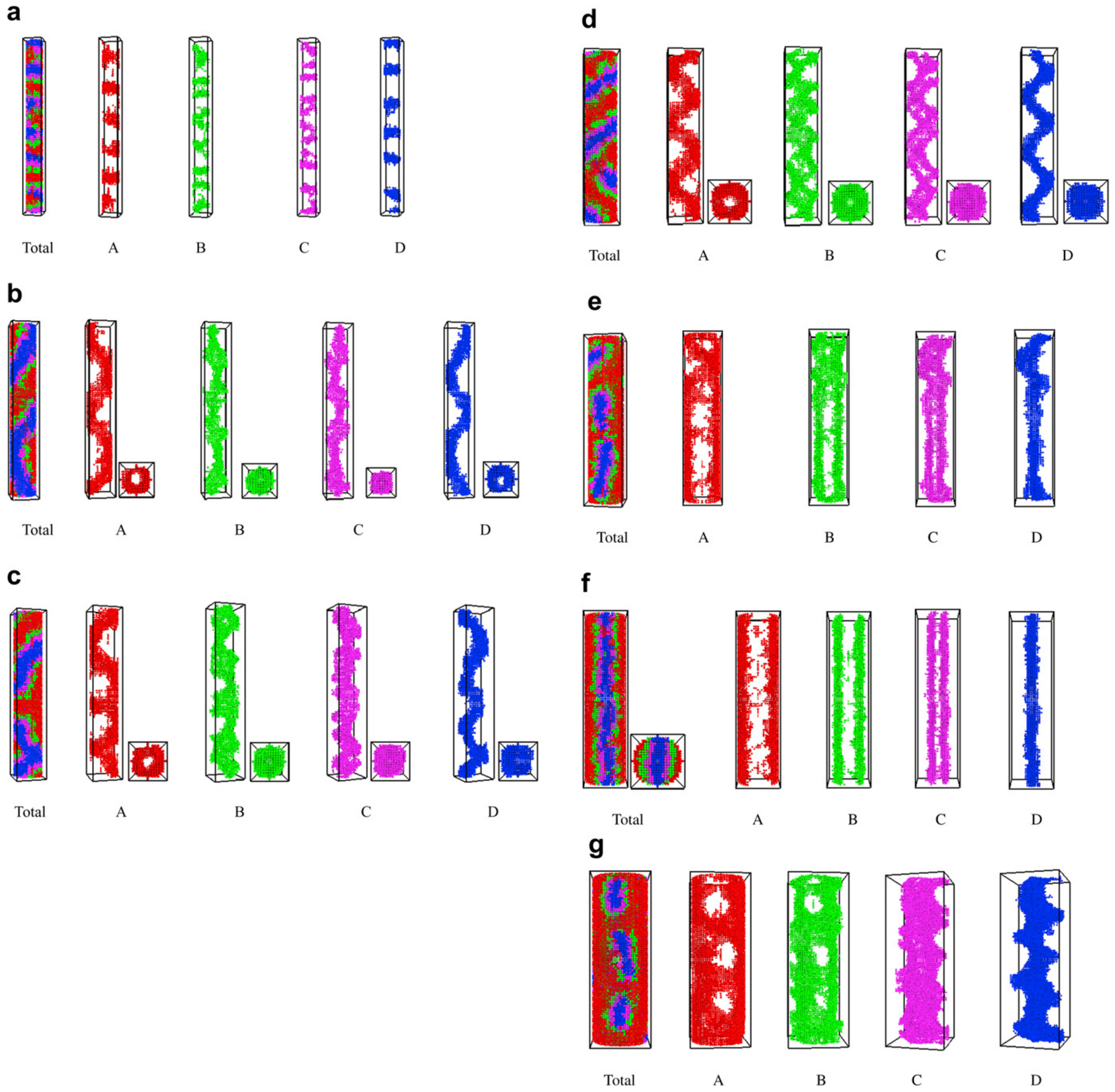

Fig. 5. Effect of the diameter of the nanopore on the morphology of the tetrablock copolymer $A_5B_5C_5D_5$ melts for $\varepsilon_{AB} = \varepsilon_{AC} = \varepsilon_{AD} = \varepsilon_{BC} = \varepsilon_{BD} = \varepsilon_{CD} = \varepsilon = 0.2\,kT$, $\varepsilon_{AA} = \varepsilon_{BB} = \varepsilon_{CC} = \varepsilon_{DD} = \varepsilon_{SS} = 0$, $\varepsilon_{AS} = \varepsilon_{BS} = \varepsilon_{CS} = \varepsilon_{DS} = \varepsilon_{WS} = 0$, $\varepsilon_{BW} = \varepsilon_{CW} = \varepsilon_{DW} = 0$, $\varepsilon_{AW} = -0.1\,kT$ and $l = 84\sigma$. (a) $d = 9\sigma$; (b) $d = 11$–13σ; (c) $d = 15\sigma$; (d) $d = 17\sigma$; (e) $d = 19\sigma$; (f) $d = 21$–25σ;(g) $d = 29\sigma$.

structure with alternate stacked disks to another ordered one decreases because the “confining effect” becomes weaker.

To understand the connection between the configuration of the molecules and the morphology of the copolymer melts, we calculated the square of the radius of gyration, which is defined as follows:

$$R^2_{g,//y} = \left\langle \frac{1}{N}\sum_i (y_i - y_{com})^2 \right\rangle \quad (1)$$

$$R^2_{g,\perp y} = \left\langle \frac{1}{N}\sum_i \left[(x_i - x_{com})^2 + (z_i - z_{com})^2\right] \right\rangle \quad (2)$$

$$R^2_{g} = \left\langle \frac{1}{N}\sum_i \left[(x_i - x_{com})^2 + (y_i - y_{com})^2 + (z_i - z_{com})^2\right] \right\rangle \quad (3)$$

where, $(R_{g,\ //y}/\sigma)^2$, $(R_{g,\ \perp y}/\sigma)^2$ and $(R_g/\sigma)^2$ stand for the square radius of gyration of the copolymer in the y direction (in this paper, the y direction is the cylindrical axis), the square radius of gyration of the copolymer along the normal to the y direction, and the square radius of gyration of the copolymer in the three dimensional space, respectively. x_i, y_i, and z_i represent the coordinates of the ith segment; x_{com}, y_{com}, and z_{com} represent the coordinates of the center of mass of the polymer chain, and N is the total number of segments in the chain.

Fig. 4 present the square radius of gyration of $A_5B_5C_5D_5$ as a function of the diameter of the nanopore for $\varepsilon_{AB} = \varepsilon_{AC} = \varepsilon_{AD} = \varepsilon_{BC} = \varepsilon_{BD} = \varepsilon_{CD} = \varepsilon$. $(R_{g,\ \perp y}/\sigma)^2$ and $(R_{g,\ //y}/\sigma)^2$ provide the orientation of the tetrablock copolymer chains. As the diameter of the nanopore increases, $(R_{g,\ \perp y}/\sigma)^2$, $(R_{g,\ //y}/\sigma)^2$ and $(R_g/\sigma)^2$ change very little for $\varepsilon = 0.10kT$ (Fig. 4a), but they change much more for $\varepsilon = 0.25kT$ (Fig. 4b). For $\varepsilon = 0.10kT$, a small change of the square radius of gyration does not induce any change in the morphology as the diameter of the cylindrical nanopore is varied (See Fig. 2). The calculations show that $(R_{g,\ //y}/\sigma)^2 > (R_{g,\ \perp y}/\sigma)^2$ in all the cases considered in Fig. 4a. This indicates that the copolymer is preferentially directed along the y direction of the nanopore than along the normal to the y direction. However, for $\varepsilon = 0.25kT$, as the diameter of the nanopore increases, $(R_{g,\ \perp y}/\sigma)^2$ first increases, thus forcing the morphology of the copolymer melt to change from stacked disks to a mixed phase containing stacked disks and single helixes, to a phase of single helixes of each of the A and D segments plus double helixes of each of the B and C segments; further, $(R_{g,\ \perp y}/\sigma)^2$ decreases leading to stacked disks; it increases again and phases containing helixes are generated (See Fig. 2). $(R_{g,\ //y}/\sigma)^2$ has the opposite behavior; and $(R_g/\sigma)^2$, generally, increases as the diameter of the nanopore increases.

The copolymer chains are preferentially directed along the y direction than along the normal to the y direction in nanopores of small diameters. By increasing the diameter, they become preferentially directed along the normal to the y direction than along the y direction; later, they become again preferentially directed along the y direction than along the normal to the y direction, and further, preferentially directed along the normal to the y direction than along the y direction. These results indicate that morphology transitions occur when the configuration of the polymer changes. A morphology consisting of stacked disks is generated when the copolymer chains are preferentially directed along the y direction than along the normal to the y direction, whereas morphologies containing helixes form when the copolymer chains are preferentially directed along the normal to the y direction than along the y direction. Hence, the configuration of the polymer chains plays a key role in the morphology of the copolymer melts.

3.2. Attractive surfaces

Fig. 5 presents the morphologies of a tetrablock copolymer as a function of the diameter d of a cylindrical nanopore for $\varepsilon_{AB} = \varepsilon_{AC} = \varepsilon_{AD} = \varepsilon_{BC} = \varepsilon_{BD} = \varepsilon_{CD} = \varepsilon = 0.2\,kT$, $\varepsilon_{AA} = \varepsilon_{BB} = \varepsilon_{CC} = \varepsilon_{DD} = \varepsilon_{SS} = 0$, $\varepsilon_{AS} = \varepsilon_{BS} = \varepsilon_{CS} = \varepsilon_{DS} = \varepsilon_{WS} = 0$, $\varepsilon_{BW} = \varepsilon_{CW} = \varepsilon_{DW} = 0$, $\varepsilon_{AW} = -0.1\,kT$ and $l = 84\sigma$. For the small diameter $d = 9\sigma$, a distorted stacked disks structure is generated by each of the segments due to the attractive interaction between the A segments and the surface of the nanopore. As the diameter of the nanopore increases to $d = 11$ or 13σ, distorted helixes are generated by each of the segments. The helixes are nearer to the surface of the pore for the segments A and D. For $d = 15\sigma$, the structure is similar to that for $d = 13\sigma$, with the difference that the helix is nearer to the surface of the nanopore only for the A segments. For $d = 17\sigma$, the segments A, B, and D generate single helixes, whereas segment C generates a double helix. For $d = 19\sigma$, a mixed phase of helixes and lamellae parallel to the pore axis is formed by each of the segments. For $d = 21\sigma$ to 25σ, each of the segments generates lamellae parallel to the nanopore axis in the sequence ABCDDCBA. For $d = 29\sigma$, a structure with perforated curved lamellae for each of the A and the B segments and with fins for each of the C and D segments is generated.

Comparing the morphologies of the systems without and with interactions between A segments and the surface of a nanopore, we find that helixes are formed for smaller nanopore diameters in the latter. This means that the attractive interactions between segments and the surface of the nanopore play an important role in the morphology build up.

To examine the relation between morphology and configuration of the molecules, the square of the radius of gyration and of its components in the parallel and normal directions to the pore axis are plotted for the $A_5B_5C_5D_5$ molecules of Fig. 5 versus d/σ in Fig. 6. $(R_{g,\ \perp y}/\sigma)^2$ first increases and $(R_{g,\ //y}/\sigma)^2$ decreases as the diameter of the nanopore increases, and this changes the morphology from stacked disks to single helixes. Because $(R_{g,\ \perp y}/\sigma)^2$ is larger than $(R_{g,\ //y}/\sigma)^2$, helixes are formed for $d = 17\sigma$. Further, as the diameter increases up to 25σ, the difference between $(R_{g,\ \perp y}/\sigma)^2$ and $(R_{g,\ //y}/\sigma)^2$ becomes increasingly larger and the morphology acquires a lamellae structure parallel to the axis of the nanopore. For $d = 29\sigma$, $(R_{g,\ \perp y}/\sigma)^2$ slightly decreases and $(R_{g,\ //y}/\sigma)^2$ slightly increases, and the morphology acquires the structure in Fig. 5(g).

Figs. 7 and 8 present, respectively, the morphologies and radii of gyration of a tetrablock copolymer as a function of the diameter of

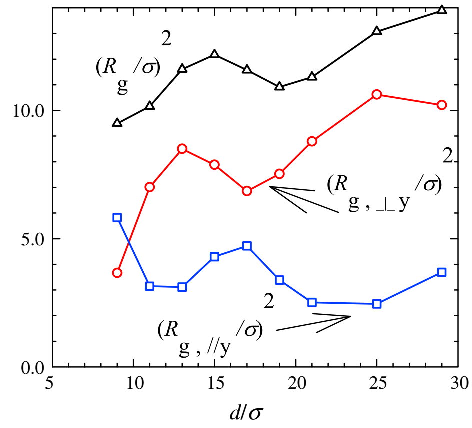

Fig. 6. Square radius of gyration of $A_5B_5C_5D_5$ for $\varepsilon_{AB} = \varepsilon_{AC} = \varepsilon_{AD} = \varepsilon_{BC} = \varepsilon_{BD} = \varepsilon_{CD} = \varepsilon = 0.2\,kT$, $\varepsilon_{AA} = \varepsilon_{BB} = \varepsilon_{CC} = \varepsilon_{DD} = \varepsilon_{SS} = 0$, $\varepsilon_{AS} = \varepsilon_{BS} = \varepsilon_{CS} = \varepsilon_{DS} = \varepsilon_{WS} = 0$, $\varepsilon_{BW} = \varepsilon_{CW} = \varepsilon_{DW} = 0$, $\varepsilon_{AW} = -0.1\,kT$and $l = 84\sigma$.

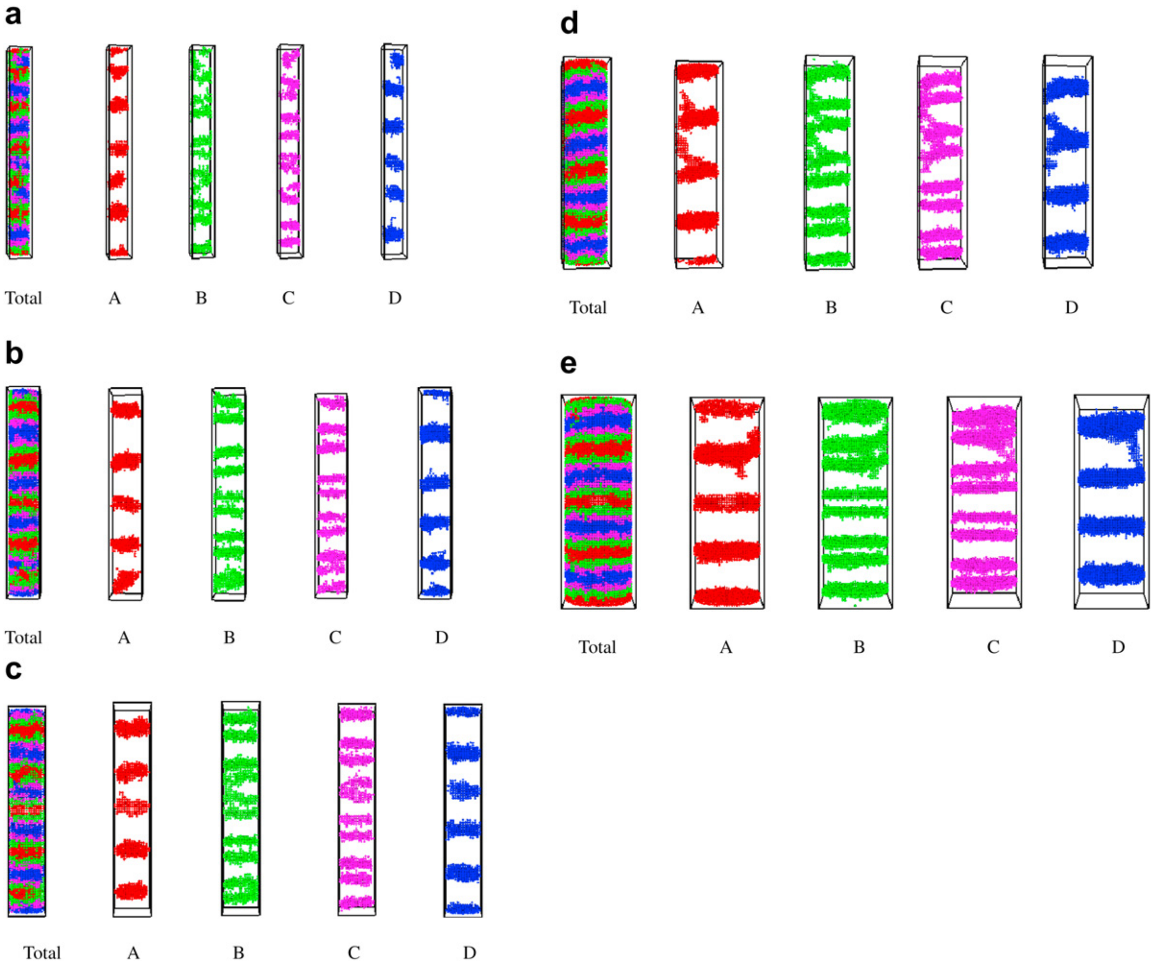

Fig. 7. Effect of the diameter of the nanopore on the morphology of the tetrablock copolymer $A_5B_5C_5D_5$ melts for $\varepsilon_{AB} = \varepsilon_{AC} = \varepsilon_{AD} = \varepsilon_{BC} = \varepsilon_{BD} = \varepsilon_{CD} = \varepsilon = 0.2\,kT$, $\varepsilon_{AA} = \varepsilon_{BB} = \varepsilon_{CC} = \varepsilon_{DD} = \varepsilon_{SS} = 0$, $\varepsilon_{AS} = \varepsilon_{BS} = \varepsilon_{CS} = \varepsilon_{DS} = \varepsilon_{WS} = 0$, $\varepsilon_{AW} = \varepsilon_{CW} = \varepsilon_{DW} = 0$, $\varepsilon_{BW} = -0.1\,kT$ and $l = 84\sigma$. (a) $d = 9$–11σ; (b) $d = 13\sigma$; (c) $d = 15\sigma$; (d) $d = 17$–25σ; (g) $d = 29\sigma$.

the cylindrical nanopore when the B segments (and not the A segments) are attracted by the surface of the pore. Both $(R_{g,\,//y}/\sigma)^2$ and $(R_{g,\,\perp y}/\sigma)^2$ are almost constant, but the former is always larger than the latter. As a result, most morphologies acquire a stacked disks structure. The length L_p of the repeat unit of the stacked disks increases as the diameter d increases. It has values between 14σ for $d = 9$–11σ, and 16.8σ for $d = 13$–15σ. For $d = 29\sigma$ (Fig. 7e), a centrosymmetric stacked disks phase with the sequence ABCDDCBA and period $L_p = 21\sigma$ is formed.

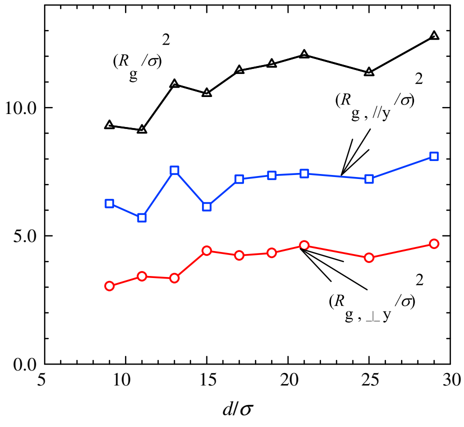

Fig. 8. Square radius of gyration of $A_5B_5C_5D_5$ for $\varepsilon_{AB} = \varepsilon_{AC} = \varepsilon_{AD} = \varepsilon_{BC} = \varepsilon_{BD} = \varepsilon_{CD} = \varepsilon = 0.2\,kT$, $\varepsilon_{AA} = \varepsilon_{BB} = \varepsilon_{CC} = \varepsilon_{DD} = \varepsilon_{SS} = 0$, $\varepsilon_{AS} = \varepsilon_{BS} = \varepsilon_{CS} = \varepsilon_{DS} = \varepsilon_{WS} = 0$, $\varepsilon_{AW} = \varepsilon_{CW} = \varepsilon_{DW} = 0$, $\varepsilon_{BW} = -0.1\,kT$and $l = 84\sigma$.

Figs. 5–8 indicate that the attractive interactions between different segments of the copolymer and the surface of the nanopore affect differently the components of the radius of gyration of the molecules, as well as the morphologies of the copolymer melts.

4. Conclusion

In conclusion, the morphologies of tetrablock copolymer ABCD melts and their configurations when they are confined in cylindrical nanopores were investigated by lattice Monte Carlo simulations. The effects of the nanopore diameter, of the repulsive interactions between different kinds of segments, and of the attractive interactions between one kind of segments and the surface of the nanopore on the morphology of a copolymer melt and on its configuration were investigated. For a neutral wall of the nanopore, a transition from disordered to an ordered phase occurs, at a repulsive energy between different segments of the copolymer of about $0.10kT$. Above this critical value, a centrosymmetric stacked disks phase with the sequence ABCDDCBA is first formed; further, other ordered morphologies are generated. Cases in which in addition to the repulsive interactions between different kinds of segments, there is also attraction between the surface of the nanopore and one kind of segments are also investigated. We found that the configuration of the polymer chain plays a key role in the morphology of a copolymer melt. A morphology with stacked disks is generated when the copolymer chain are preferentially directed along the nanopore axis, whereas a morphology containing helixes or lamellae parallel to the axis of the nanopore is formed when the copolymer chain are preferentially directed normal to the nanopore axis. The nature of the segment which is attracted by the nanopore surface also affects the morphology of the polymer.

Acknowledgments

We wish to thank the Center for Computational Research of the State University of New York at Buffalo for the computer time provided.

References

[1] Shin K, Xiang HQ, Moon SI, Kim T, McCarthy TJ, Russell TP. Science 2004;306:76.
[2] Xiang H, Shin K, Kim T, Moon SI, McCarthy TJ, Russell TP. Macromolecules 2004;37:5660.
[3] Xiang H, Shin K, Kim T, Moon SI, McCarthy TJ, Russell TP. Macromolecules 2005;38:1055.
[4] He X, Song M, Liang H, Pan C. J Chem Phys 2001;114:10510.
[5] Chen P, He X, Liang H. J Chem Phys 2006;124:104906.
[6] Li W, Wickham RA, Garbary RA. Macromolecules 2006;39:806.
[7] Li W, Wickham RA. Macromolecules 2006;39:8492.
[8] Sevink GJA, Zvelindovsky AV, Fraaije JGEM, Huinink HP. J Chem Phys 2001;115:8226.
[9] Sevink GJA, Zvelindovsky AV. J Chem Phys 2008;128:084901.
[10] Yu B, Sun P, Chen T, Jin Q, Ding D, Li B, et al. Phys Rev Lett 2006;96:138306.
[11] Feng J, Liu HL, Hu Y. Macromol Theory Simul 2006;15:674.
[12] Wu Y, Cheng G, Katsov K, Sides SW, Wang J, Tang J, et al. Nat Mater 2004;3:816.
[13] Feng J, Ruckenstein E. J Chem Phys 2006;125:164911.
[14] Feng J, Ruckenstein E. Macromolecules 2006;39:4899.
[15] Feng J, Ruckenstein E. J Chem Phys 2007;126:124902.
[16] Feng J, Ruckenstein E. J Chem Phys 2008;128:074903.
[17] Chen P, Liang H. J Phys Chem B 2008;112:1918.
[18] Chen H, Ruckenstein E. J Chem Phys 2009;130:024901.
[19] Chen H, Ruckenstein E. J Chem Phys 2009;131:114904.
[20] Chen H, Ruckenstein E. Langmuir 2009;25:12315.
[21] Curgul S, Van Vliet KJ, Rutledge GC. Macromolecules 2007;40:8483.
[22] Takahashi K, Hasegawa H, Hashimoto T, Bellas V, Iatrou H, Hadjichristidis N. Macromolecules 2002;35:4859.
[23] Takano A, Soga K, Asari T, Suzuki J, Arai S, Saka H, et al. Macromolecules 2003;36:8216.
[24] Jaffer KM, Wickham RA, Shi AC. Macromolecules 2004;37:7042.
[25] Larson RG, Scriven LE, Davis HT. J Chem Phys 1985;83:2411.
[26] Reiter J, Edling T, Pakula T. J Chem Phys 1990;93:837.
[27] Feng J, Ruckenstein E. Macromol Theory Simul 2002;11:630.